Eur. Phys. J. Appl. Phys. **51**, 30602 (2010)
DOI: 10.1051/epjap/2010114

THE EUROPEAN PHYSICAL JOURNAL APPLIED PHYSICS

Regular Article

Infrared antenna array based on nano-holes in ultrathin metallic films

D. Li, Z.J. Zhang, F. Gao, Z. Wang, R.H. Fan, L.Y. Sun, R.L. Zhang, and R.W. Peng[a]

National Laboratory of Solid State Microstructures and Department of Physics, Nanjing University, Nanjing 210093, P.R. China

Received: 18 May 2010 / Accepted: 9 June 2010
Published online: 2 August 2010 –

Abstract. In this work, we investigate the emission of the nano-hole array in an ultrathin silver film at infrared regime. It is shown that when the incident light illuminates the nano-hole array, the localized surface plasmons are excited and serve as electric dipoles. The emission of the nano-hole array presents a strong directivity. The maximum radiation is located at infrared regime, and it can be tuned by the period of the nano-hole array, the incidence angle and the polarization of the excitation light. These findings extend our understandings of optical property of metallic nano-structures and provide a unique way to achieve infrared antenna arrays, which may achieve potential applications in photovoltaics and telecommunication.

1 Introduction

The tremendous efforts to develop radar and related techniques during World War II resulted not only in the technologies for military use, but also in a great body of information and new techniques in the electronics and high-frequency fields. Among these techniques, antenna is a key component to convert electromagnetic radiation into localized energy and vice versa in radio and microwave frequencies. As the wavelength of electromagnetic wave shifts to optical regime, lenses and mirrors are traditionally used to modify the transformation of light. Can we apply the concept of antenna to optical and infrared regimes, so we can collect and enhance optical energy locally and increase the efficiency of photovoltaic device? The major obstacles seem to be nano-manufacture with sufficient precision and identification of specific antenna. Recently as the development of nano-fabrications, optical antennas have been experimentally realized [1–5]. Besides, effective wavelength scaling for optical antennas has been theoretically explored [6]. However, most works on optical antenna reported so far focus on electromagnetic radiation of metallic nano-rods and nano-particles, where surface plasmon plariton (SPP) is involved [7]. Very recently, Alaverdyan et al. have made the nano-hole chains effectively behave as linear wire antennas [8], and Zhang et al. have successfully realized plasmonic antenna array at visible frequency made by nanoaperatures [5]. As a matter of fact, since Ebbesen et al. [9] reported the extraordinary optical transmission through an array of sub-wavelength holes perforated on silver film, much attention has been paid to the optical properties of nanoscopic apertures [10–15]. However, less attention has been paid to infrared antenna and infrared antenna array based on nanoapertures.

In this work, we demonstrate that the array of nano-holes in ultrathin silver films can radiate at infrared frequency and serve as an infrared antenna array. It is shown that when the incident light shines the nano-hole array, the localized surface plasmons (LSPs) are excited and serve as electric dipoles. The emission of the nano-hole array presents a strong directivity and is sensitive to the polarization of incident light. When a transverse-electric (TE) light illuminates the nano-hole array in silver films, maximum radiation of the array is independent of the incident angle, yet it red-shifts as the array rotates in-plane. When a transverse-magnetic (TM) light illuminates the nano-hole array, the optical radiation can be tuned by both the incident angle and the in-plane rotation. These findings provide a way to construct infrared antenna arrays, and may have potential applications in photovoltaics and telecommunication.

2 The sample fabrication and optical measurement

In the experiment, the silver film with the thickness of 50 nm was coated on the substrate of optical glass by magnetron sputtering technique. Then, with focused-ion-beam facility (strata FIB 201, FEI company, 30 keV Ga ions), the array of holes was fabricated on the silver film. Scanning-electron microscope (SEM) measurements (Fig. 1a) indicate that the samples were well fabricated as designed, the period of the holes in the array was about $a = 580$ nm, and the diameter of the hole was about $d = 300$ nm.

Optical transmission of the silver films perforated nano-holes has been measured by PerkinElmer Lambda 900 spectrophotometer in the range from 400 nm to 2500 nm when the incident beam is perpendicular to the

[a] e-mail: rwpeng@nju.edu.cn

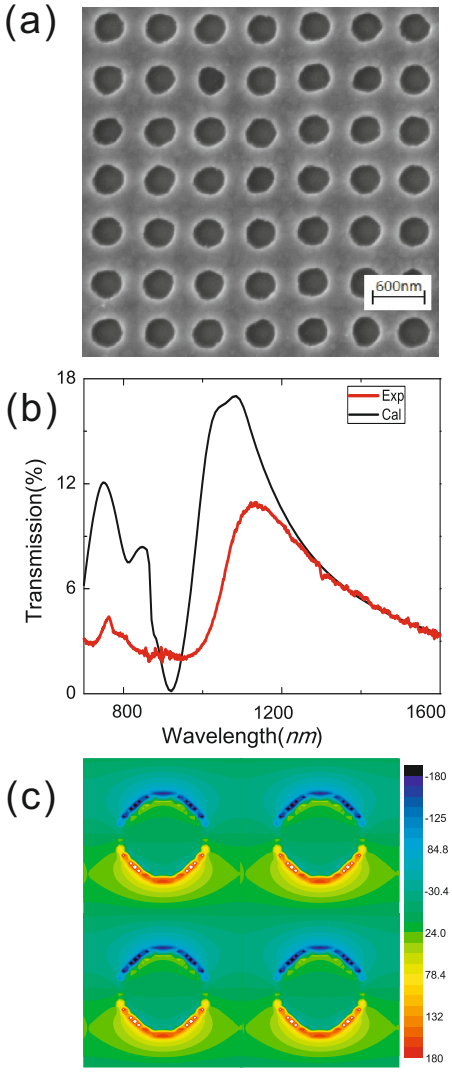

Fig. 1. (Color online) (a) The field-emission scanning electronic microscope (SEM) image of the array of apertures perforated on 50 nm-thick silver film, where the period of apertures in the square lattice is $a \cong 580$ nm, and the diameter of the aperture is $d \cong 300$ nm. (b) The measured and calculated optical transmission spectra of the silver film with aperture array when the incident beam is perpendicular to the film. (c) The distribution of charge density on the bottom surface of silver film, which corresponds to the transmission peak at $\lambda_0 \cong 1150$ nm. Positive and negative charges accumulate separately on the opposite bank of the aperture.

film. Figure 1b shows the measured and calculated optical transmission spectra of the silver film with aperture array, which are in excellent agreement. The main transmission peak appears at about twice of the lattice periodicity, i.e., $\lambda_0 \cong 1150$ nm $\cong 2a$, which completely deviates from the SPP-involved extraordinary optical transmission [10,13] of $\lambda_{\max} = a/\sqrt{i^2+j^2}\sqrt{\varepsilon_D\varepsilon_M/(\varepsilon_D+\varepsilon_M)}$. (Here, ε_M and ε_D are the permittivities of the metal and the dielectric, respectively. And i, j are both integers.) In the calculation, three-dimensional (3D) full-vector finite-difference time-domain (FDTD) method is applied. The frequency-dependent permittivity of silver is based on the Lorentz-Drude model [16]. Periodic boundary condition is set for in-plane boundaries and perfectly-matched layer is set for the perpendicular boundary. The grid spacing is carefully chosen to guarantee convergence in calculations. In addition to the optical properties, we also investigate the charge density distribution [17] in the aperture array at the wavelength corresponding to the maximum transmission (λ_0). It is found that the positive and negative charges accumulate separately on the opposite bank of the aperture (Fig. 1c), forming dipoles oscillating coherently with the incident light.

The microscopic process around each aperture can be understood as follows: by illumination, the local electric field drives free electrons on the surface of ultrathin film to oscillate. Yet the movement of charges is blocked on the edge of each nano-hole, generating the LSPs around the nano-hole. And the LSPs serve as electric dipoles. Actually, the dipoles are induced by the local electric field, which includes the following three parts: the incident electric field, the field created by the other induced dipoles in the array, and the field contributed by the propagating surface plasmons (PSPs) [5]. The dipoles oscillate with the frequency of incident light. Note that each oscillating dipole radiates, hence the array of nano-apertures actually performs as a planar antenna array. The radiation of the dipole array originates from the coherent superposition of the emission of the dipoles. Since the dipoles are induced by the local electric field, the radiation of the dipole array is related to the incident field, the other induced dipoles, and the PSPs. Generally, the in-plane electric field of the TM incidence will initiate dipoles oscillating, and it will influence the radiation as the incident angle increases. The induced dipoles will interact with each other and the interaction as well as the radiation will change when the sample is rotated in-plane. Besides, the PSPs will affect the radiation for the TM mode of electromagnetic wave since the PSPs are usually excited in this case.

3 The theoretical analysis on the far-field emission of nano-hole arrays

Consider the far-field emission of a rectangular array of $N_x \times N_y$ oscillating dipoles (nano-apertures), which locates at x-y plane and has a spatial periodicity (a_x, a_y). For generality, we let the dipole array being illuminated obliquely with incident angle θ_0 and in-plane angle ϕ_0. The far-field receiver locates at $R(r, \theta, \phi)$. (Here $r \gg a_x$ and $r \gg a_y$.) The electric field at $R(r, \theta, \phi)$ is contributed by the emission of all dipoles, and it follows

$$\left|\vec{E}\right|^2 = \left|\vec{E}_0 f_x f_y\right|^2 \propto \frac{\sin^2\delta}{\lambda^4}\frac{\sin^2(N_x\alpha)}{\sin^2\alpha}\frac{\sin^2(N_y\beta)}{\sin^2\beta}, \quad (1)$$

where $\vec{E}_0$ is the electric field emitted by the dipole $\vec{P}_0 = P_0 e^{-i\omega t}\hat{e}_p$ at the origin of x-y plane (the point O), and $f_{x(y)}$ is the array factor. According to antenna theory, the

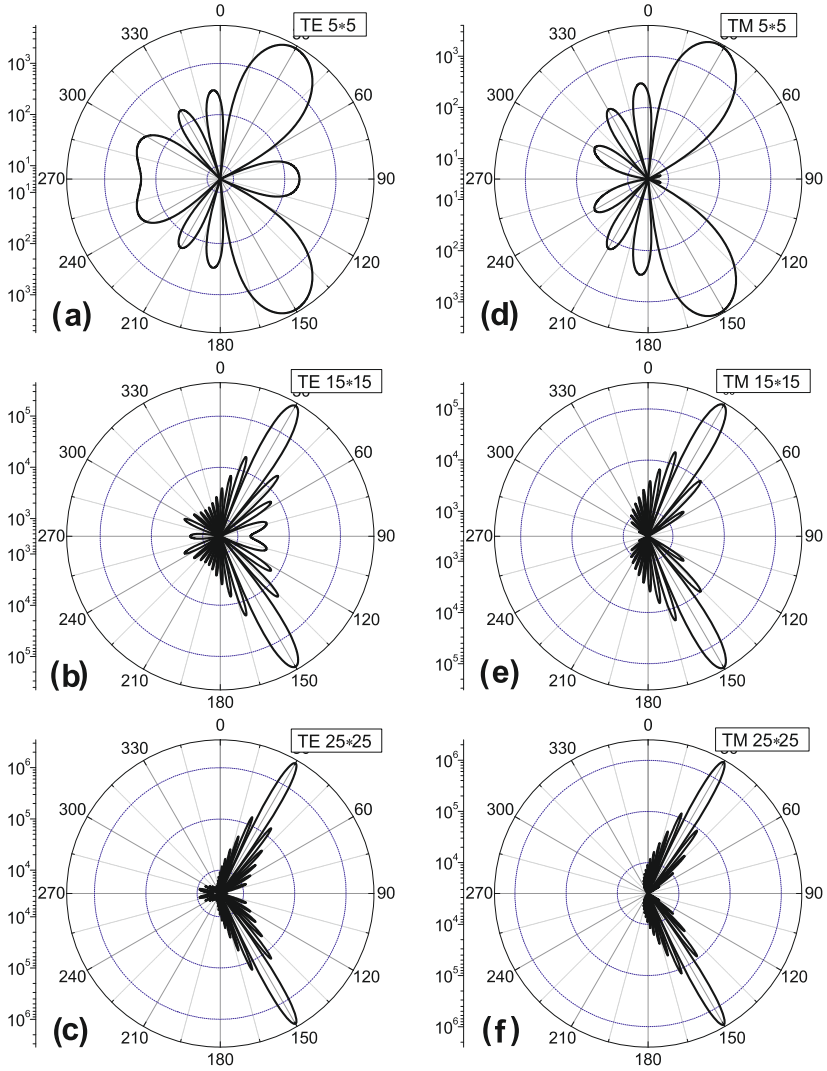

Fig. 2. The calculated far-field E-plane patterns for the arrays of (a) 5×5 dipoles, (b) 15×15 dipoles, and (c) 25×25 dipoles excited by TE incidence at $\lambda_0 \cong 1150$ nm. And the calculated far-field E-plane patterns for the arrays of (d) 5×5 dipoles, (e) 15×15 dipoles, and (f) 25×25 dipoles excited by TM incidence at $\lambda_0 \cong 1150$ nm.

electric field $\vec{E}_0$ can be expressed as

$$\vec{E}_0 = \frac{P_0}{4\pi c^2 \varepsilon_0} \frac{1}{r} (-\omega^2) e^{-i\omega(t-r/c)} \sin\delta \hat{e}_\delta, \qquad (2)$$

where $\omega = 2\pi c/\lambda$ is the radiation frequency, and $\hat{e}_\delta$ is the unit vector perpendicular to $\overrightarrow{\mathrm{OR}}$ and is within the plane of $\vec{P}_0$ and $\overrightarrow{\mathrm{OR}}$. δ is the angle between the dipole $\vec{P}_0$ and $\overrightarrow{\mathrm{OR}}$, therefore, for TE incidence $\sin\delta = 1$, and for TM incidence $\sin\delta = \sin\theta$. In equation (2), c is vacuum light velocity, and ε_0 is vacuum dielectric constant. Meanwhile, the array factor $f_{x(y)}$ arises from the phase shifts (α and β) of dipole emissions along x and y directions, respectively, i.e., $\alpha = \pi a_x/\lambda(\sin\theta\cos\phi - \sin\theta_0\cos\phi_0)$ and $\beta = \pi a_y/\lambda(\sin\theta\sin\phi - \sin\theta_0\sin\phi_0)$.

The far-field emission pattern for the planar dipole array has been calculated in both TE and TM incidences, respectively (as shown in Figs. 2a–2c and Figs. 2d–2f). The major features of a planar dipole array can be identified from equations (1) and (2). First, the emission field shown in equation (1) possesses the form of sinc function ($f(x) = \sin x/x$), and it has a maximum at $x = 0$, which corresponds to $\theta = \theta_0$ and $\phi = \phi_0$ simultaneously. Therefore, the radiation of the array has a maximum along original incident direction. Second, the emission field shown in equation (1) is a function of $\sin\theta\cos\phi$ and $\sin\theta\sin\phi$, so the radiation of the dipole array possesses a strong directivity [18]. Third, the maximum radiation depends on the polarization ($\sin\delta$ in Eq. (2)), the angle of incident light (θ_0) and also the in-plane rotation of dipole array (ϕ_0).

4 The measured far-field emission of nano-hole arrays

Now we study the far-field optical spectra of the nano-aperture array with different polarization of incident light, incident angles and in-plane array rotation, respectively.

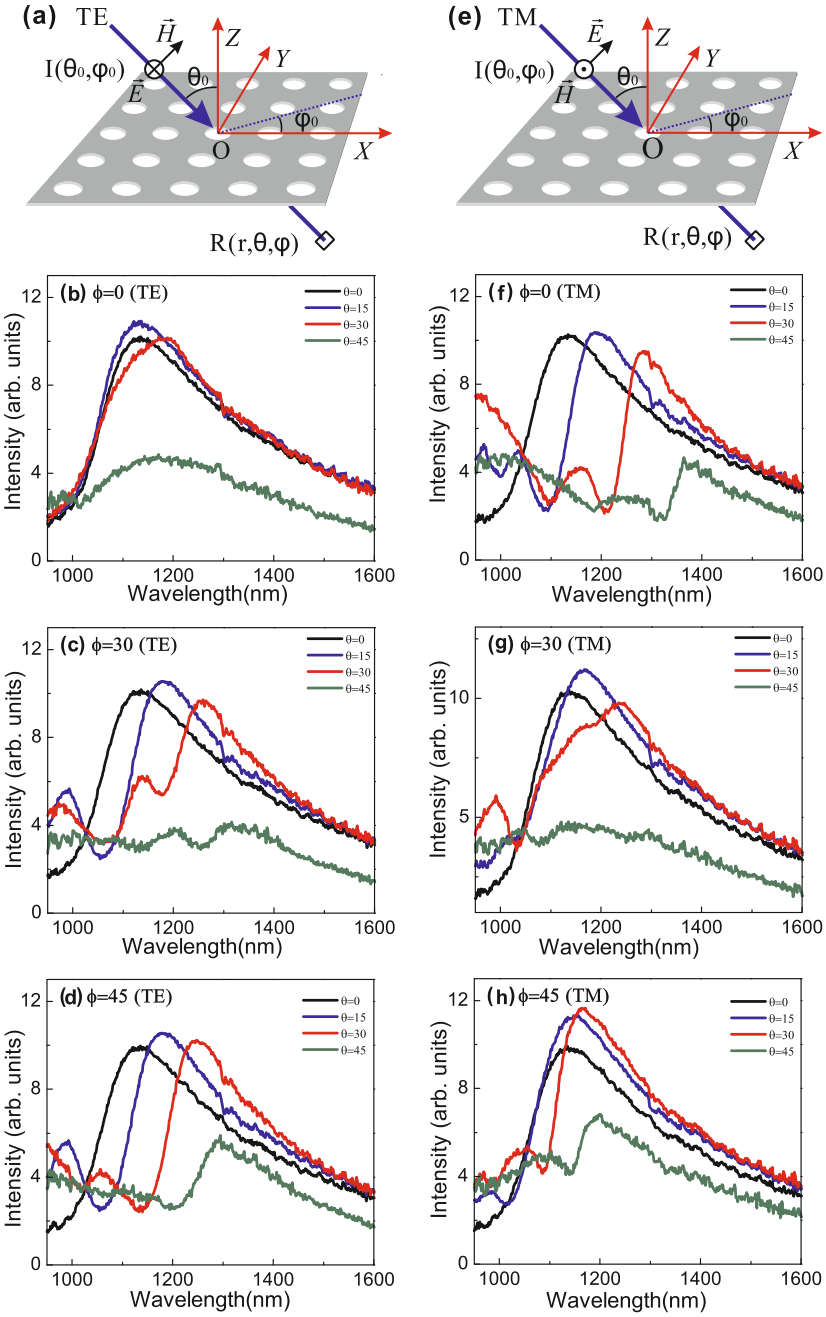

Fig. 3. (Color online) The schematic configurations of the (a) TE and (e) TM incidence on the sample, respectively. The experimental optical spectra detected at the far field $R(r, \theta_0, \phi_0)$, i.e., $\theta = \theta_0$ and $\phi = \phi_0$, when the TE and TM lights illuminate the periodic array of apertures perforated on the 50 nm-thick silver film. The periodicity of apertures in the square lattice is $a \cong 580$ nm, and the diameter of the aperture is $d \cong 300$ nm. In the case of $\phi = \phi_0 = 0$: (b) TE, and (f) TM. In the case of $\phi = \phi_0 = 30°$: (c) TE and (g) TM. In the case of $\phi = \phi_0 = 45°$: (d) TE, and (h) TM.

The array contains 100×100 holes with period $a_x = a_y \equiv a \cong 580$ nm. The diameter of the hole is controlled to $d \cong 300$ nm. As schematically shown in Figures 3a and 3e, the light with TE mode and TM mode illuminates on the array, respectively. The incident angle θ_0 varies and the array can be rotated in-plane. The optical detector locates at far-field $R(r, \theta_0, \phi_0)$, i.e., $\theta = \theta_0$ and $\phi = \phi_0$.

When a TE light illuminates the nano-aperture array, the measured optical spectra are shown in Figures 3b–3d. In the case of $\phi_0 = 0$, the radiation peak appears at $\lambda_0 \cong 1150$ nm $\cong 2a$, which remains even if the incident angle θ_0 is changed (as shown in Fig. 3b). It is known that the diffraction edges for a dipole array give rise to a strong dipolar interaction [19]. At the normal incidence ($\theta_0 = 0$ and $\phi_0 = 0$), the diffraction edges are given by $\lambda = [(i/a_x)^2 + (j/a_y)^2]^{-1/2}$, where i, j are both integers and denote the grating diffraction order. Thereafter, the corresponding resonances occur at the wavelength which is

no longer than the array period. Therefore in our system, the wavelength of $\lambda_0 = 2a$ is not the diffraction edge at the normal incidence. Actually, when a TE light illuminates the nanoaperture array on silver film, there is no excitation of PSPs on surface [12]. However, the LSPs [20] can be excited around each aperture; thereafter, a plasmonic dipole is formed across each nanoaperture. This phenomenon is similar to the case at visible frequency [5]. Physically, the dipole is induced by both the incident electric field and the field created by the other induced dipoles in the array. When TE light obliquely illuminates the nanoaperture array, the incident electric field always lies in plane of the nanoapertures and keeps identically even if the incidence angle varies. As a result, the distribution of plasmonic dipoles in the array remains and the directivity of the radiation is kept at different incidence angles (as shown in Fig. 3b). However, the situation varies if $\phi_0 \neq 0$. For a nonvanishing ϕ_0, the moment of each dipole (P_0) remains for different incident angle, yet the orientation of the dipoles in the array is rotated. Therefore, the array factor $f_{x(y)}$ in equation (1) varies when the incident angle is changed. Consequently, the directivity of the dipole antenna is changed, the maximum radiation shifts to lower frequency, and its intensity decreases as the incident angle θ_0 is increased, as shown in Figures 3c and 3d. Therefore, the optical emission of nano-aperture array can be tuned by the incident angle and the in-plane rotation of array in the TE incidence.

We also investigated the optical spectra when TM mode of electromagnetic wave illuminates the nanoaperture array, as shown in Figures 3f–3h. Obviously, for $\phi_0 = 0$, the radiation peak can be found, but maximum radiation red-shifts as the incident angle θ_0 is increased (Fig. 3f). It is known that when TM mode illuminates the apertures perforated on silver film, both LSP and PSP can be excited on the surface. The role of PSP in our system is twofold. On one hand, PSP modifies the charge accumulation around the apertures, which eventually affects the electrical dipole moment P_0 in equation (2). On the other hand, the momentum of PSP will modulate the array factor $f_{x(y)}$ in equation (1) by adding the wave vector of PSP to the in-plane wave vector of the incident light. Therefore, as the incident angle θ_0 increases, maximum radiation shifts (Fig. 3f). For a nonvanishing ϕ_0, the radiation peak also red-shifts and the radiation decreases as the incident angle θ_0 is increased, as shown in Figure 3g. A special case occurs at $\phi_0 = 45°$. As shown in Figure 3h, the radiation peak appears approximately at $\lambda_0 \cong 1150$ nm $\cong 2a$, suggesting that the maximum radiation shifts only slightly when the incident angle θ_0 is increased. We therefore confirm that for TM incident light, the influence of PSP on optical spectra can be observed, where the maximum radiation is significant tuned by the incident angle and the in-plane rotation of array.

5 Summary

In summary, we have investigated the emission of the nano-hole array in an ultrathin silver film at near-infrared frequency. It is demonstrated that the LSPs are excited and serve as electric dipoles when the incident light illuminates the nano-hole array. The emission of the nano-hole array presents a strong directivity. The maximum radiation is located at infrared region, and it can be tuned by the in-plane rotation of the nano-hole array and the excitation light. The investigation provides a way to construct infrared antenna arrays, and may have potential applications in photovoltaics and telecommunication.

This work was supported by grants from the National Natural Science Foundation of China (Grant Nos. 10625417 and 10874068), the State Key Program for Basic Research from the Ministry of Science and Technology of China (Grant Nos. 2010CB630705 and 2006CB921804), and partly by Jiangsu Province (Grant No. BK2008012).

References

1. P. Mühlschlegel, H.-J. Eisler, O.J.F. Martin, B. Hecht, D.W. Pohl, Science **308**, 1607 (2005)
2. R.D. Grober, R.J. Schoellkopf, D.E. Prober, Appl. Phys. Lett. **70**, 1354 (1997)
3. D.P. Fromm, A. Sundaramurthy, P.J. Schuck, G. Kino, W.E. Moerner, Nano Lett. **4**, 957 (2004)
4. J.S. Shumaker-Parry, H. Rochholz, M. Kreiter, Adv. Mater. **17**, 2131 (2005)
5. Z.J. Zhang, R.W. Peng, Z. Wang, F. Gao, X.R. Huang, W.H. Sun, Q.J. Wang, Mu Wang, Appl. Phys. Lett. **93**, 171110 (2008)
6. L. Novotny, Phys. Rev. Lett. **98**, 266802 (2007)
7. H.S. Zhou, I. Honma, H. Komiyama, J.W. Haus, Phys. Rev. B **50**, 12052 (1994)
8. Y. Alaverdyan, B. Sepúlveda, L. Eurenius, E. Olsson, M. Käll, Nat. Phys. **3**, 884 (2007)
9. T.W. Ebbesen, H.J. Lezec, H.F. Ghaemi, T. Thio, P.A. Wolff, Nature (London) **391**, 667 (1998)
10. W.L. Barnes, A. Dereux, T.W. Ebbesen, Nature (London) **424**, 824 (2003)
11. F.J. García de Abajo, J.J. Sáenz, Phys. Rev. Lett. **95**, 233901 (2005)
12. C. Genet, T.W. Ebbesen, Nature (London) **445**, 39 (2007)
13. Z.H. Tang, R.W. Peng, Z. Wang, X. Wu, Y.J. Bao, Q.J. Wang, Z.J. Zhang, W.H. Sun, Mu Wang, Phys. Rev. B **76**, 195405 (2007)
14. Y.J. Bao, R.W. Peng, D.J. Shu, Mu Wang, X. Li, J. Shao, W. Lu, N.B. Ming, Phys. Rev. Lett. **101**, 087401 (2008)
15. F. Gao, D. Li, R.W. Peng, Q. Hu, K. Wei, Q.J. Wang, Y.Y. Zhu, Mu Wang, Appl. Phys. Lett. **95**, 011104 (2009)
16. A.D. Rakić, A.B. Djurišić, J.M. Elazar, M.L. Majewski, Appl. Opt. **37**, 5271 (1998)
17. X.R. Huang, R.W. Peng, Z. Wang, F. Gao, S.S. Jiang, Phys. Rev. A **76**, 035802 (2007)
18. E.A. Wolff, *Antenna analysis* (Artech House, Norwood, 1988)
19. M. Meier, A. Wokaun, P.F. Liao, J. Opt. Soc. Am. B **2**, 931 (1985)
20. A. Degiron, H.J. Lezec, N. Yamamoto, T.W. Ebbesen, Opt. Commun. **239**, 61 (2004)